ISTITUTO NAZIONALE DI FISICA NUCLEARE

Sezione di Milano

INFN/AE-93/24
12 Novembre 1993

F.W. Bopp, R. Engel, I. Kawrakow, D. Pertermann, J. Ranft:

MINIJETS IN THE TWO-COMPONENT DUAL PARTON MODEL IN HADRONIC AND HEAVY ION COLLISIONS

PACS. No.: 13.85.Hd; 13.85.Ni; 12.38.Mk; 12.40.Aq; 12.40.Lk

Servizio Documentazione
dei Laboratori Nazionali di Frascati

INFN - Istituto Nazionale di Fisica Nucleare
Sezione di Milano

INFN/AE–93/24
12 Novembre 1993

MINIJETS IN THE TWO–COMPONENT DUAL PARTON MODEL IN HADRONIC AND HEAVY ION COLLISIONS

F.W.Bopp,[a] R.Engel, I.Kawrakow, D.Pertermann[b] and J.Ranft[c]
Presented by J.Ranft at LBL–Workshop on Pre–equilibrium Parton Dynamics in Heavy Ion Collisions, Berkeley, Sept.1 1993.

[a]Fachbereich Physik, Universität Siegen, D–57068 Siegen, F.R.G.

[b]Fachbereich Physik, Universität Leipzig, D–04109, Leipzig, F.R.G.

[c]INFN, Sezione di Milano, Via Celoria 16, I–20133 Milano, Italy

We use new fits to parton structure functions, including structure functions with Lipatov behaviour at small x–values and discuss the minijet component in the two–component Dual Parton Model with a supercritical Pomeron as demanded by the fits to cross section data. We find, that a consistent model can only be formulated with a $p_{\perp thr}$ cut–off increasing with enery. The implications for particle production in hadronic and heavy ion collisions are discussed.

1. Introduction

Soft multiparticle production characterizing hadronic and heavy ion interactions energies cannot be understood purely within theoretical approaches provided by perturbative QCD. The nonperturbative soft component of hadron production, which is responsable for all of hadron production at low energies is still present at present and future collider energies. I know, that this statement contradicts some of the other contributions to this Workshop, therefore, I will point to my arguments as I present the material.

Using basic ideas of the dual topological unitarization scheme[1,2] the Dual Parton Model (DPM) (a recent review is given in Ref.[3]) has been very successfully describing soft hadronic processes. Several new features of $p\bar{p}$ collisions at collider energies as

well as of heavy–ion collisions at CERN energies, which were subsequently confirmed by experiments, could be anticipated.

Observations like rapidity plateaus and average transverse momenta rising with energy, KNO scaling violation, transverse momentum–multiplicity correlations and *minijets* pointed out, that soft and hard processes are closely related. These properties were understood within the two–component Dual Parton Model.[4–9] The hard component is introduced applying lowest order of perturbative hard constituent scattering.[10] Single diffraction dissociation, which is not essential for heavy ion collisions, is represented by a triple–Pomeron exchange (high mass single diffraction) and a low mass component.

The Monte–Carlo implementation of the Dual Parton Model (DTUJET[5] for hadron–hadron collisions and DTUNUC[11] and DPMJET[12] for hadron–nucleus and heavy ion collisions) enables us to investigate the predictions given by the model at energies of present and future hadron and heavy ion colliders. In the present paper we discuss mainly the minijet component. This is appropriate, since the first results from HERA on deep inelastic scattering at low x[13] seem to indicate, that the structure functions at low x rise much stronger than anticipated in the past by most of the conventional structure function parametrizations. We will see, that this, if also found for the gluon structure function, can lead to dramatic consequences for the minijet component.

2. The two–component Dual Parton Model

The soft input cross section in our unitarization scheme is described by the supercritical Pomeron

$$\sigma_s = g^2 s^{\alpha(0)-1} \tag{1}$$

with g being the effective proton–Pomeron coupling constant and $\alpha(0)$ the Pomeron intercept. The corresponding Pomeron–trajectory is given by $\alpha(t) = \alpha(0) + \alpha' t$. The supercritical Pomeron was used in the two–component DPM from the beginning,[4] while the corresponding efforts in the USA use the critical Pomeron with $\alpha(0) = 1$ from Durand and Pi[14] up to HIJING.[15] A large part of the differences between HIJING and the DPM–results is due to this different starting point. In all fits of the Pomeron parameters to cross section data including the ones, I will report here, we get consistently better fits with the supercritical Pomeron than with the critical one, we have always done both fits and occasionally reported also our fits using the critical Pomeron. *These better fits to the supercritical Pomeron are one of my arguments for the continuous presence of the soft component to multiparticle production in the TeV energy region.* Furthermore we introduce graphs with Pomeron–Pomeron couplings. Provided that the Pomeron–Pomeron coupling constant Γ is small in comparison with other couplings, such as g, it is sufficient to consider the expansion in Γ only up to first order[5] . Thus a correction to the pure Pomeron–exchange is represented by the triple–Pomeron graph (Fig. 1(c)). The simplest cut of the triple–Pomeron (Fig. 1(c)) corresponds to a high mass single diffractive interaction. High mass diffraction is a comparable rare process. High mass means that the diffractively excited system should not be a well defined hadron resonance. We also describe high mass double diffractive processes again to first order introducing loop graphs (Fig. 1(d)).

The input cross section for semihard multiparticle production σ_h is calculated applying the QCD improved parton model as described in Ref..[16, 4, 7, 8]

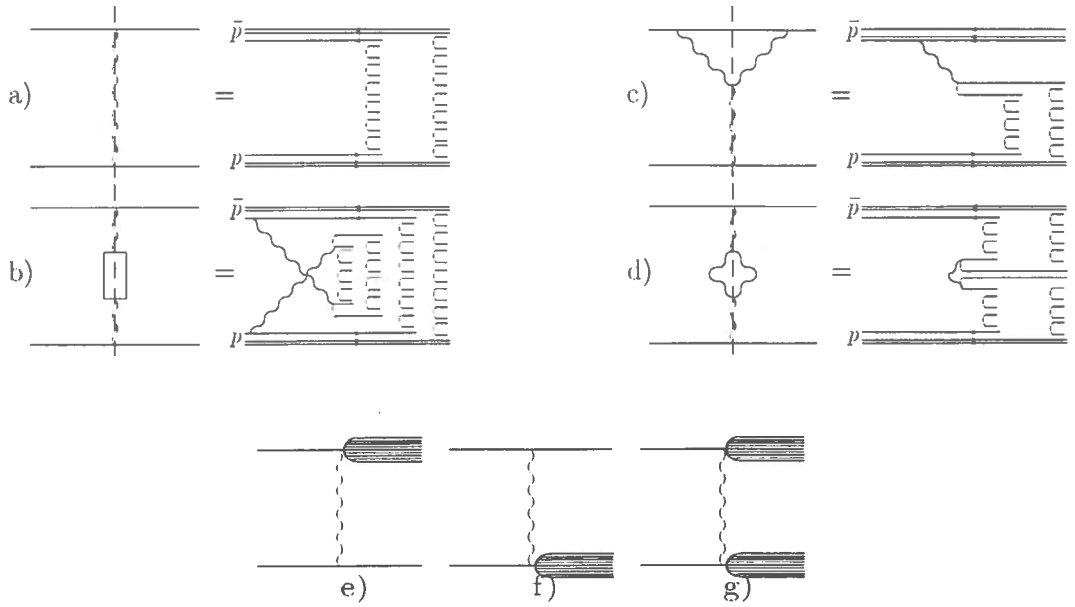

Figure 1. Diagrams and the corresponding cut graphs for the exchange of a) one soft Pomeron, b) one hard Pomeron, and c) one triple–Pomeron (high mass single diffraction). Fig. d) shows one cut Pomeron–loop graph (high mass double diffraction). Low mass single diffractive processes (e),(f) and low mass double diffractive processes (g) are introduced via a two–channel eikonal formalism

$$\sigma_h = \sum_{i,j} \int_0^1 dx_1 \int_0^1 dx_2 \int d\hat{t}\ \frac{1}{1+\delta_{ij}} \frac{d\sigma_{QCD,ij}}{d\hat{t}}\ f_i(x_1,Q^2) f_j(x_2,Q^2)\ \Theta(p_\perp - p_{\perp thr}) \tag{2}$$

$f_i(x,Q^2)$ are the structure functions of partons with the flavor i and scale Q^2 and the sum i,j runs over all possible flavors. To remain in the region where perturbation theory is valid, we use a low $p_\perp$ cut–off $p_{\perp_{thr}}$ for the minijet component. Furthermore, since we calculate $\sigma_{QCD,ij}$ in lowest-order QCD perturbation theory we multiply the hard input cross section σ_h with a K factor in the range of 1.5 to 2. A hard interaction leads to a chain system shown in Fig. 1(b).

The momentum fractions of the constituents at the ends of the different chains are sampled using the exclusive parton distribution, which has the form for an event with n_s soft and $n_h (n_h \geq 1)$ hard Pomerons

$$\rho(x_1,...,x_{2n_s},...,x_{2n_s+2+n_h}) \sim \frac{1}{\sqrt{x_1}} \Big(\prod_{i=3}^{2n_s+2} \frac{1}{x_i}\Big) x_2^{1.5} \prod_{i=2n_s+3}^{2n_s+2+n_h} g(x_i,Q_i)\,\delta\Big(1 - \sum_{i=1}^{2n_s+2+n_h} x_i\Big). \tag{3}$$

The distributions $g(x_i,Q_i)$ are the distribution functions of the partons engaged in the hard scattering.

Soft(s), hard(h), high mass single diffractive(TP), and high mass double diffractive(L) processes are treated simultaneously within an eikonal unitarization scheme using the impact parameter representation

$$\chi_i(B,s) = \frac{\sigma_i(s)}{8\pi b_i} \exp[-\frac{B^2}{4b_i}], \qquad i = s,h,TP,L \tag{4}$$

normalized by

$$\int 2\chi_i(B,s)\,d^2B = \sigma_i \tag{5}$$

with $b_h = b, b_s = b_{TP} = b_L = b + \alpha' log(s)$ and $b = 3.52\ GeV^{-2}$ (see Ref.[5]). The exclusive cross section for l_c cut soft Pomerons, m_c cut hard Pomerons, n_c cut triple–Pomeron graphs and p_c cut loop graphs is given by

$$\sigma(l_c, m_c, n_c, p_c, B, s) = \frac{(2\chi_s)^{l_c}}{l_c!}\frac{(2\chi_h)^{m_c}}{m_c!}\frac{(-2\chi_{TP})^{n_c}}{n_c!}\frac{(-2\chi_L)^{p_c}}{p_c!}\exp[-2\chi(B,s)] \tag{6}$$

with

$$\chi(B,s) = \chi_s(B,s) + \chi_h(B,s) - \chi_{TP}(B,s) - \chi_L(B,s). \tag{7}$$

The total and elastic cross section are given by

$$\sigma_{tot} = 4\pi\int_0^\infty BdB(1-\exp[\chi(B,s)]),\quad \sigma_{el}(B,s) = \frac{1}{4}[\sigma_{tot}(B,s)]^2. \tag{8}$$

3. Current parametrizations of parton structure functions

During 1992–3 new data on deep inelastic scattering and new fits to parton structure functions were reported. New features of these fits include (i) the flavor dependence of sea–quark distributions and (ii) a stronger rise of the structure functions at low x–values, that is in the region important for minijets. These fits by Martin Roberts and Stirling[17] and by the CTEQ–Collaboration[18] include functions with a conventional $1/x$ singularity of sea–quark and gluon distributions (for instance the MRS[D–0] functions) as well as functions with a $1/x^{1.5}$ singularity (for instance the MRS[D–] functions). The present (pre–HERA) measurements do not allow to decide between these two possibilities. However, there are theoretical arguments in favor of the $1/x^{1.5}$ singularity.[19] These more singular parton distributions were in the past used to calculate the minijets,[7,8] but not taken very seriously. This has now to be changed, since the first HERA–data seem to favor just these singular parton distribution functions.[13] In Fig.2 we reproduce the relevant Figure from the HERA–H1–Collaboration,[13] in Fig.3 we presen the MRS[D–0] and MRS[D–] functions for gluons. Gluons are the most important source of minijets, unfortunately, so far no HERA data for the gluon distributions are available, but we should start now to discuss the implementation of the more singular functions for minijets.

4. Determining the free parameters of the model in fits to cross–section data

4.1. DTUJET92, energy independent cut–off $p_{\perp,thr}$

We describe these fits and the resulting model[7,8] without much detail and we restrict our discussion to the fits concerning the new structure function sets MRS[D–0] and MRS[D–].[17] For both considered parton distributions we obtained an acceptable description of the data. In Fig. 4 we compare the calculated cross sections to the data from ISR to Tevatron energies.[7,8] The fit results show that $\alpha(0)$ always corresponds to a supercritical soft Pomeron. Due to the uncertainties of the parton distributions at low x-values the extrapolation to high energies is rather difficult. We are not able to give an unique prediction of the behaviour of the cross sections at supercollider energies. The reason for this are the input minijet cross sections, which we calculate using the two different

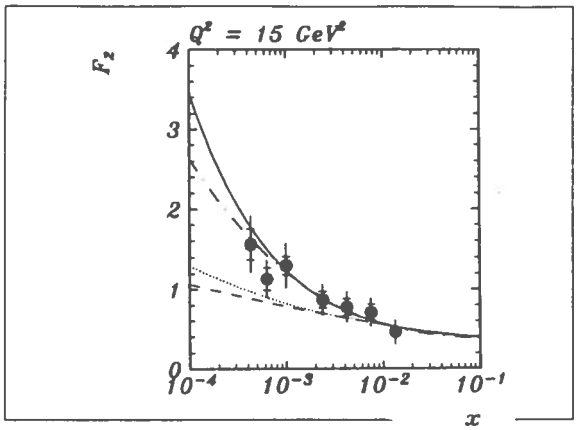

Figure 2. First HERA–H1 measurements of structure functions at small x.[13]

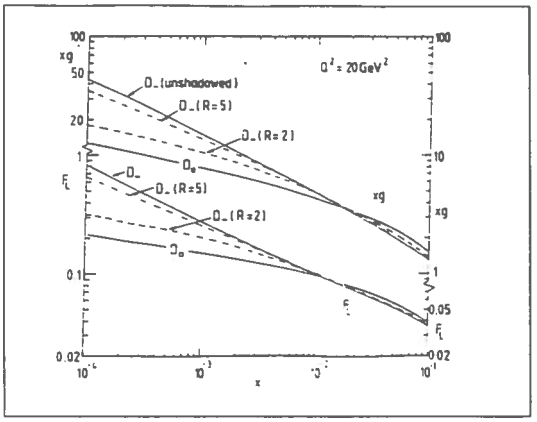

Figure 3. Gluon distributions in the small x–region according to the last MRS–fit.[17]

parton distributions: We obtain at $\sqrt(s)$ = 40 TeV approximately with MRS[D–0] σ_h = 200 mb and with MRS[D-] σ_h =1200 mb. The unitarization method compensates for most of the difference and gives output values of σ_{tot} of about 120 and 160 mb, respectively. If we calculate the rapidity distributions in the two models the differences are much bigger. In Fig.5 we plot the central pseudorapidity plateau as function of the energy for the two models, up to present collider energies both models agree with each other and with the experimental data but in the super collider energy region the differences are very big. For heavy ion collisions at CERN–LHC energies, we expect, that MRS[D-] would give a plateau 50 percent higher than expected with conventional structure functions.[12]

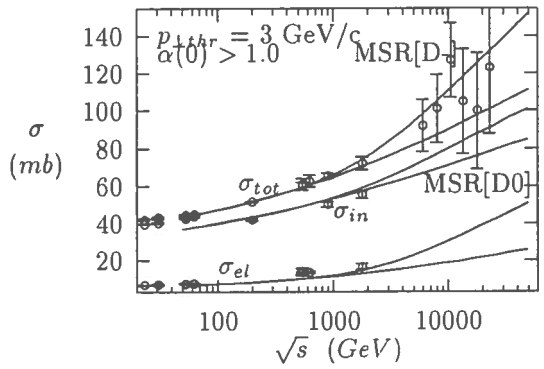

Figure 4. Cross sections σ_{tot}, σ_{el}, and σ_{in} , compared with the two-component DPM DTUJET92.[7]

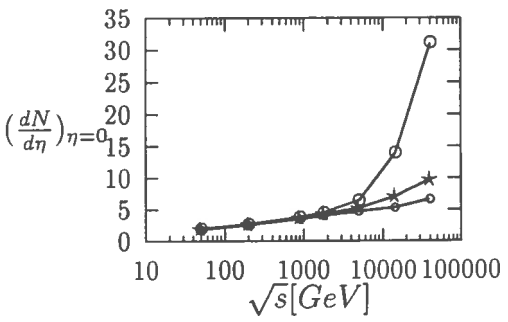

Figure 5. Rise of the pseudorapidity plateau in DTUJET92

At present CERN and TEVATRON collider energies, there is nothing wrong with this model and indeed, DTUJET92, with JETSET[20] fragmentation and parton evolution gives with all MRS-92 and CTEQ PDF's an excellent phenomenology. We have compared to data: charged particle pseudorapidity distributions, $p_\perp$-distributions, $E_\perp$-distributions, π^0 production in the fragmentation region, correlations between $p_\perp$ and $dN/d\eta$ etc.

At these energies the model is still consistent, since the minijet cross sections are small. However, extrapolating with MRS[D–] to LHC and SSC energies, the model becomes inconsistent and produces unreliable results like a pseudorapidity plateau at SSC energies of 30-35 charged hadrons per pseudorapidity unit, while previous versions of the model and the same model with conventional PDF's give plateaus between 6 and 8.

At these energies and with the MRS[D–] structure function DTUJET92 has become inconsistent and is wrong.

What is inconsistent and wrong: The input minijet cross sections σ_h, which we put so far into the unitarization scheme are inclusive cross sections normalized to $n_{minijets}\sigma_{inel}$, where $n_{minijets}$ is the multiplicity of minijets. But the physical processes, which contribute to this inclusive cross section, if we use parton distributions with Lipatov behaviour, are $2 \to n$ parton processes. $2 \to n$ processes give a contribution to σ_h equal to $n\sigma_{2\to n}$. Furthermore, the s–channel iteration of such a huge cross section is probably incorrect. What we should really use in the unitarization, but what we do not know how to compute reliably at present would be

$$\sigma_h = \sum_n \sigma_{2\to n} \tag{9}$$

4.2. DTUJET93, energy dependent cut–off $p_{\perp,thr}$

The way to remove this inconsistency is to make in DTUJET-93 the threshold for minijet production $p_{\perp thr}$ energy dependent in such a way, that at no energy and for no PDF the resulting σ_h is bigger than the total cross section. Then at least we have a cross section, which is indeed mainly the cross section of a $2 \to 2$ parton process at this level, but we can get back to the real $2 \to n$ processes via parton showering. One possible form for this energy dependent cut off is:

$$p_{\perp thr} = 2.5 + 0.12[\lg_{10}(\sqrt{s}/\sqrt{s_0})]^3 \quad [GeV/c], \quad \sqrt{s_0} = 50GeV. \tag{10}$$

The resulting σ_h are smaller than the total cross sections resulting after the unitarization for all MRS-92 and CTEQ PDF's and also the older KMRS[21] distributions. We note, that this energy dependent $p_\perp$ cut–off corresponds numerically closely to the one used by Geiger,[22–24] but the physical motivation for its use is of course completely different.

Now we are again consistent.

We use as first described in[16] at $p_{\perp thr}$ the continuity requirement for the *soft* and *hard* chainend $p_\perp$ distributions. Physically, this means, that we use the soft cross section to cut the singularity in the minijet $p_\perp$ distribution. But note, that this cut moves with rising collision energy to higher and higher $p_\perp$ values. This procedure has besides cutting the singularity more attractive features: (i)The model results (at least as long as we do not violate the consistency requirement described above) become largely independent from the otherwise arbitrary $p_\perp$ cut–off. This was already demonstrated with DTUJET90[5] and cut–offs of 2 and 3 GeV/c. (ii)The continuity between soft and semihard physics is emphasized, there is no basic difference between soft and semihard chains besides the technical problem, that perturbative QCD allows only to calculate the semihard component. (iii) With this continuity in mind we feel free to call all chainends, whatever their

origin, minijets, as soon as their $p_\perp$ exceeds a certain value, say 2 GeV/c. We turn now

Table 1
DTUJET93 model parameters obtained with a energy dependent $p_{\perp thr}$.

PDF set	$g^2(mb)$	$\alpha(0)$	α'	b	b_h	λ
MRS[D–0]	49.14	1.0636	0.173	1.63	4.01	0.565
MRS[D–]	55.96	1.0490	0.351	1.038	2.01	0.584
CTEQ[1M]	50.85	1.0589	0.210	1.516	3.44	0.562
CTEQ[1MS]	52.25	1.0560	0.256	1.365	2.96	0.574
CTEQ[1ML]	53.73	1.0489	0.250	1.390	2.83	0.529
CTEQ[1DIS]	49.85	1.0616	0.188	1.583	3.75	0.565
CTEQ[1L]	49.56	1.0614	0.208	1.520	3.81	0.593

to the fit of the Pomeron parameters in the case of DTUJET93 with the energy dependent $p_\perp$ cut–off given above. To describe the high energy particle production we have to determine the free parameters of the model, i.e. the proton-Pomeron coupling constant g, the effective soft Pomeron intercept $\alpha(0)$, the slope of the Pomeron trajectory α', the slope parameters b and b_h and the excitation coupling constant λ. This has been done by a global fit to all available data of total, elastic, inelastic, and single diffractive cross sections in the energy range from ISR to collider experiments as well as to the data on the elastic slopes in this energy range. Since there are large differences in the hard parton distribution functions at small x values resulting in different hard input cross sections we have to perform separate fits for each set of parton distribution functions.

We get again good fits using all of the PDF's, which also as before give us a supercritical Pomeron, not a critical one. In Table 1 we give the parameters obtained in the fit. All the values obtained for $\alpha(0)$ demonstrate again that the fits result in a supercritical Pomerom. In Figs. 6 and 7 we plot the fitted cross sections obtained with the MRS–92 PDF's together with the data, the fits with the CTEQ PF's are of a similar quality. We note, that the differences of the output σ_{tot} obtained with the conventional MRS[D–0] and the Lipatov behaved MRS[D–] structure functions are much smaller than in the fit with constant $p_{\perp thr}$.

In order to demonstrate the continuity of soft and semihard chainend $p_\perp$ distributions we plot in Fig.8 at three energies the numbers of chainends with $p_\perp$ bigger than $p_{\perp thr}$ as function of $p_{\perp thr}$. The plots are given before and after the parton evolution. The curves refer to the model with the CTEQ[1ML] parton distribution.

5. Multiparticle production with DTUJET93

We get again a good phenomenology with all the known results at the CERN and TEVATRON collider.

In Fig.9 we compare the pseudorapidity distribution obtained in the model with the MRS[D–] with data at collider energies[25, 26] and give the extrapolation up to SSC–energies.

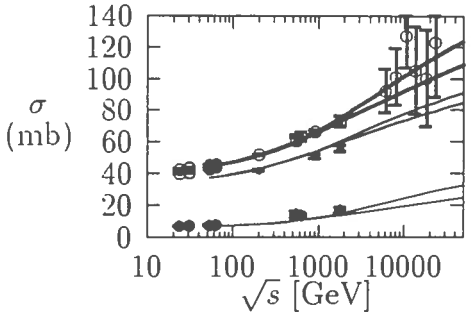

Figure 6. Cross sections σ_{tot}, σ_{el}, and σ_{in}, compared with the two-component DPM DTUJET93. (MRS[D–0] and MRS[D–])

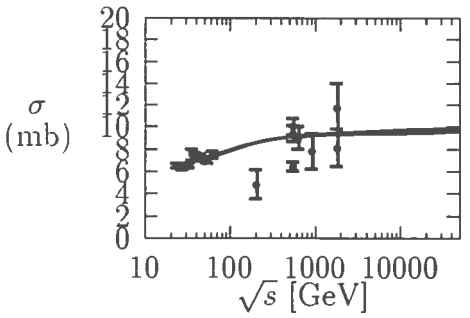

Figure 7. Cross sections σ_{diff} compared with the two-component DPM DTUJET93. (MRS[D–0] and MRS[D–])

In Fig.10 we plot the central pseudorapidity plateau obtained with DTUJET93 and the PDF's MRS[D–0], MRS[D–] and CTEQ[1ML] as function of the $\sqrt{s}$. No striking differences are seen between the three models. In Fig.11 we plot and compare to data the average transverse momenta[27] in the central rapidity region obtained with DTUJET93 and the same three PDF's. While all three models agree well with the collider data, we find striking differences in the extrapolation into the supercollider energy region: The average $p_\perp$ rises stronger for more singular PDF's.

In Fig.12 we compare transverse momentum distributions and in Fig.13 we compare transverse energy distributions with data.[27] In both Figs. The model is DTUJET93 with the CTEQ[1ML] PDF.

In Fig.14 finally we compare $p_\perp$–multiplicity correlations with data,[28] where we get good agreement for pions and antiprotons, for antiprotons the average transverse momenta rise much more strongly than for pions. the model is DTUJET93 with the MRS[D–] PDF.

We might conclude this Section: extrapolating to LHC and SSC energies, we get charged plateaus of 6–7 particles per pseudorapidity unit for the models with all MRS-92 and CTEQ PDF's. However, the average transverse momenta in the models with the singular PDF's rises more steeply than in previously published versions of DTUJET. We find at SSC energies an average $p_\perp$ typically 100 to 150 MeV/c bigger than previously.

6. Minijets in heavy ion collisions

The Dual Parton Model for processes with nuclear targets and projectiles, in the approximation with only single pomeron exchange in each elementary hadron–nucleon collision in the nucleus and with a full formation zone intranuclear cascade has been compared recently to data from hadron–nucleus and nucleus–nucleus collisions.[11, 29] This model is implemented in the in the event generator DTUNUC.

Here we use the combined model,[12] which implements in each hadron–nucleon collision inside the nucleus multiple soft and hard chains like in hadron–hadron collisions as described by the two–component Dual Parton Model[5]. This Monte–Carlo event gener-

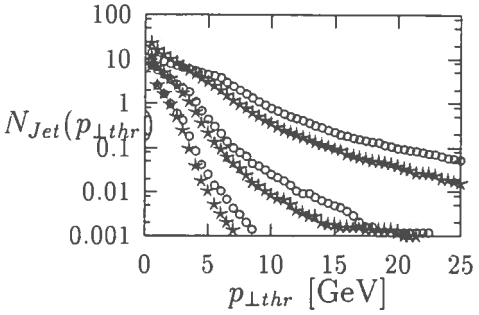

Figure 8. Number of jets with $p_\perp \geq p_{\perp thr}$, DTUJET93 with CTEQ[1ML].($\sqrt{s}$ = 50,200 and 1800 GeV)

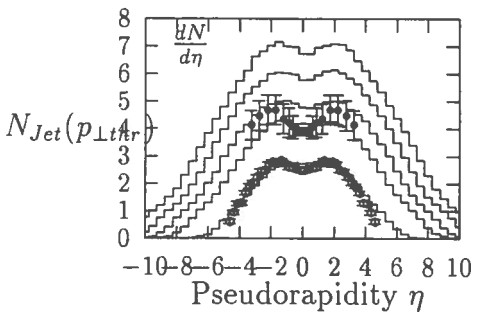

Figure 9. Pseudorapidity distributions in DTUJET93 with MRS[D−], compared to collider data[25,26] and extrapolated to TeV energies .

ator is implemented in the code DPMJET. Besides multiple soft and hard chains, like in the DTUJET Monte Carlo, DPMJET uses the Glauber model cascade in the formulation.

Furthermore, DPMJET has the following features: (i) A full formation zone suppressed intranuclear cascade is handled like in DTUNUC, i.e. all generations of secondary interactions with spectator nucleons are considered . It should however be noted, that this feature plays no role in central nucleus–nucleus collisions, where practically no spectators are left. (ii) Fermi momenta of nucleons within the interacting nuclei are introduced, together with a simple realization of Pauli's principle. (iii) To allow for the application of the model at superhigh energies a parametrization for the energy dependence of the scattering amplitude (used in the Glauber formalism) is introduced.

DPMJET can be used up to LHC energies to sample hadron–hadron, hadron–nucleus and normal and central nucleus–nucleus collisions according to the Dual Parton Model. For hadron–hadron collisions, the results from DPMJET agree to the ones obtained with the first version of DTUJET.[5]

7. Results for central heavy ion interactions

7.1. Pseudorapidity distributions in nucleus–nucleus collision

We report here on central collisions. We consider only gold (Au) nuclei as typical heavy projectiles and targets.

The rapidity and pseudorapidity distributions of hadrons in central Au–Au collisions can be understood easily from the Glauber model and the properties of hadron production in hadron–hadron collisions. In central Au+Au collisions at $\sqrt{s} = 6.3$ TeV we get about 1500 elementary nucleon–nucleon interactions. The pseudorapidity plateau in hadron–hadron collisions at this energy is about $dN/d\eta_{\eta=0} = 4 - 5$, therefore we expect in the central region of the central Au–Au collisions a rapidity plateau of 6000–7500. This is approximately, what we find in the Monte–Carlo calculation.

In Fig.15 we present the pseudorapidity distributions in central Au–Au collisions at energies from $\sqrt{s} = 20$ GeV/N to 6300 GeV/N. The plateau is found to rise much faster

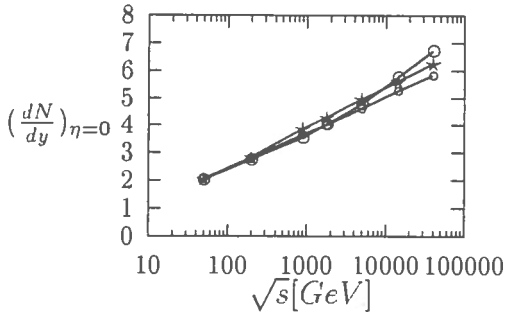

Figure 10. The rise of the central pseudorapidity plateau with energy in different DTUJET93 models .

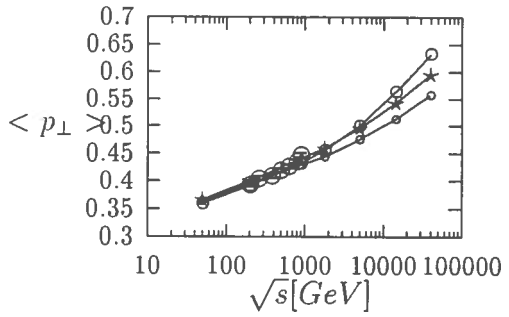

Figure 11. The rise of central average transverse momenta with energy in several DTUJET93 models, data from.[27]

with energy than in hadron–hadron collisions. The reasons for this fast rise are (i) the rise of the elementary nucleon–nucleon input cross–section in the Glauber model leading to a rise of the number of collisions N and (ii) the rising fraction of sea–sea chains which cease to be supressed kinematically with rising energy. In[12] we give for some energies two rapidity distributions in central Au–Au collisions. One distribution is without nuclear shadowing of minijets, in the second distribution nuclear shadowing is taken into account. In contrast to what was found in[15] , the differences between both curves are negligible. In the model[5] with a supercritical Pomeron most of the rise of the plateau is still due to the production of soft multiple chains in each elementary collision. Even when about 50 percent of the minijets are supressed by the nuclear shadowing, the effect on the total multiplicity and multiplicity density remains small. In,[15] a critical Pomeron is used and all the rise of the rapidity plateau in the elementary collisions is due to minijet production, therefore nuclear shadowing has an enormous effect on the multiplicity density in nucleus–nucleus collisions. We plan to introduce the new model DTUJET93 described above in the near future into DPMJET. We suppose, that the fraction of particles resulting from minijets will become bigger than in[12] and that also the influence of nuclear shadowing will rise.

7.2. Baryon stopping

In Fig. 16 we present the baryon multiplicity density as function of pseudorapidity for central Au–Au collisions at $\sqrt{s}$ = 20 to 6300 GeV/N. At $\sqrt{s}$ = 20 GeV/n we find still some finite baryon density in the central region, but starting at RHIC–energies DPMJET predicts a growing baryon free region in the central region of the collision. However, in the next version of DPMJET, using the popcorn mechanism and sea–diquark chains, enhanced baryon stopping is expected.

In our model, even if the independent production and fragmentation of hadronic chains would not break down, one step is missing so far, this is the (formation zone) cascade of produced hadrons. This step will be implemented in the future. It remains to be seen, whether the baryon free region survives this final state hadron cascade.

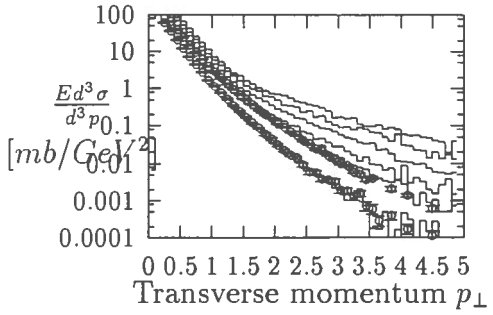

Figure 12. Comparison of transverse momentum distributions with collider data.

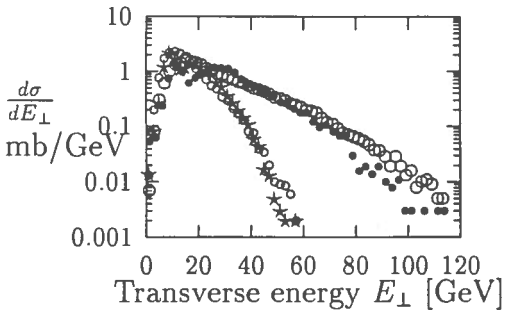

Figure 13. Comparison of transverse Energy distributions with collider data[27].

7.3. The partonic (minijet) component to the hadronic energy density in central heavy ion collisions

Two components of the energy density can be calculated separately within our model: (i)The first component is the hadronic energy density, in this component we collect the energy in form of hadronic resonances and we assume, that these resonances are born after their formation time. This component has been studied in detail in a recent paper[29]. At RHIC and the LHC we find energy densities well in the region, where the formation of a quark–gluon plasma is expected. (ii)The second component is the energy density of partons (minijets) resulting from semi–hard collisions. Only partons are included wich can have further interactions in an explicit parton cascade. This component becomes important only at LHC-energies. The number of minijets depends however crucial on the structure function used and the $p_\perp$ cutoff. This component has been studied in.[12]

In the conventional DPM the colourless strings between the partons which have participated in a hard or semihard primary nucleon–nucleon interactions are fragmented independently. In the TeV energy range of the proposed Large Hadron Collider (LHC) a very dense system of such partons may be produced and the independent string fragmentation may fail.

If we forget for the moment the slow and long range hadronisation process, we can consider these partons as free particles (at least in the first time after the interaction) moving on straight lines. Indeed, further collisions between the partons are possible. In[12] we only calculate the energy density carried by the produced minijet component. In Fig.17 we present the energy density of the minijet component at eigentimes $\tau = 1$ fm/c. The upper histograms show the results without nuclear shadowing, the lower with shadowing. As can be seen in the Figures, the nuclear shadowing reduces the density of the hard partons considerabely. Furthermore, the energy density depends crucially on the $p_\perp$ cut in contrast to the results for the final state hadrons.

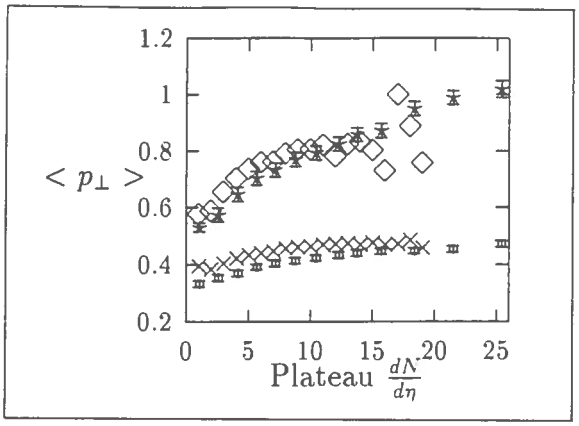

Figure 14. Comparison of average transverse momentum – multiplicity correlations with collider data.[28]

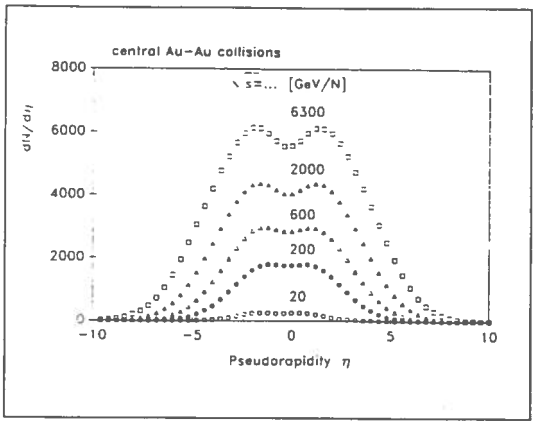

Figure 15. Pseudorapidity distribution of charged particles produced in central Au–Au collisions at different energies according to DPMJET.

8. Conclusions and summary

The two–component Dual Parton Model has some natural way to cut–off the singularity of the minijet cross section at low $p_\perp$. The model uses te soft Pomeron cross section as the low $p_\perp$ limit of the minijets.

With the new prescription in DTUJET93 we find the plateau rising like $\log s$ even with $1/x^{3/2}$ singular structure functions.

The average transverse momenta in this scheme rise more strongly with energy than in previous versions of DTUJET, In hadronic collisions, we get a satisfactory phenomenology at the energies of the CERN and TEVATRON colliders.

The new methods used in DTUJET93 will be soon used in a new version of DPMJET for heavy ion collisions at RHIC and the LHC. We expect no significant changes of the plateaus calculated in central heavy ion collisions, but the average transverse momenta are expected to rise against the present version of DPMJET.

9. Acknowledgements

One of the authors (J.R.) acknowledges useful discussions with B.Andersson, V.N.Gribov and A.B.Kaidalov.

REFERENCES

1. G. F. Chew and C. Rosenzweig, *Nucl. Phys.* B104(1976)290.
2. C. Hong-Mo, J. E. Paton and T. Sheung Tsun, *Nucl. Phys.* B86(1975)470.
3. A. Capella, U. Sukhatme, C. I. Tan and J. Tran Thanh Van, Orsay Preprint, LPTHE 92–38, to be published in Phys. Rep., 1992.
4. A. Capella, J. Tran Thanh Van and J. Kwiecinski, *Phys. Rev. Lett.* 58(1987)2015.
5. P. Aurenche, F. W. Bopp, A. Capella, J. Kwiecinski, M. Maire, J. Ranft and J. Tran Thanh Van, *Phys. Rev.* D45(1992)92.
6. F. W. Bopp, A. Capella, J. Ranft and J. Tran Thanh Van, *Z. Phys.* C51(1991)99.

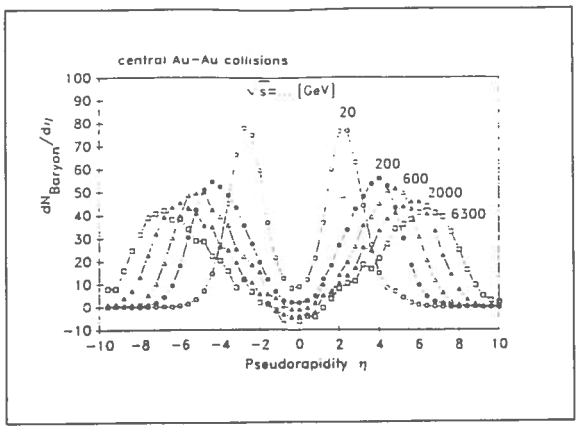

Figure 16. Pseudorapidity distribution of Baryons (sum of all kinds of baryons - sum of all kinds of antibaryons) in central Au–Au collisions at energies $\sqrt{s}$ = 20 to 6300 GeV/N. Calculated with DPMJET.

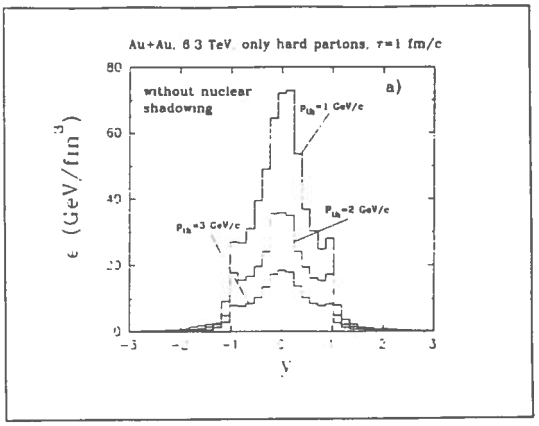

Figure 17. The energy density of the minijet component in central Au+Au collisions at $\sqrt{s}$ = 6.3 TeV at eigentime τ = 1 fm/c. The three curves correspond to $p_\perp$ cuts of 1,2 and 3 GeV/c respectively.

7. F. W. Bopp, D. Pertermann and J. Ranft, *Z. Phys.* C54(1992)683.
8. R. Engel, F. W. Bopp, D. Pertermann and J. Ranft, *Phys. Rev.* D46(1992)5192.
9. S. Roesler, R. Engel and J. Ranft, *Z. Phys.* C59(1993)481.
10. B. L. Combridge, J. Kripfganz and J. Ranft, *Phys. Lett.* 70B(1977)234.
11. H.-J. Möhring and J. Ranft, *Z. Phys.* C52(1991)643.
12. I.Kawrakow, H.–J.Möhring and J.Ranft, *Phys. Rev.* D47(1993)3849.
13. Abt, T. et al.,H1–Collaboration, DESY preprint DESY 93–117, subm. to Nucl.Phys.B,, 1993.
14. J. Durand and H. Pi, *Phys. Rev. Lett.* 58(1987)2015.
15. X. N. Wang and M. Gyulassy, *Phys. Rev.* D44(1991)3501.
16. K. Hahn and J. Ranft, *Phys. Rev.* D41(1990)1463.
17. A. D. Martin, R. G. Roberts and W. J. Stirling, *Phys. Rev.* D47(1993)867.
18. J.Botts et al., CTEQ–Collaboration, to be published in Phys. Lett. B, 1993.
19. E.M.Levin, to be publ. in Proc. of Aachen Conf. "QCD – 20 years later" , 1992.
20. T. Sjöstrand, CERN Report CERN–TH.6488/92, 1992.
21. J. Kwiecinski, A. D. Martin, R. G. Roberts and W. J. Stirling, *Phys. Rev.* D42(1990)3645.
22. Geiger, K., *Phys. Rev.* D46(1992)4965.
23. Geiger, K., *Phys. Rev.* D46(1992)4986.
24. Geiger, K., *Phys. Rev.* D47(1993)133.
25. G. J. Alner et al., UA5 Collab., *Z. Phys.* C33(1986)1.
26. F. Abe et al., CDF Collab., *Phys. Rev.* D41(1990)2330.
27. C. Albajar et al., *Nucl. Phys.* B 335(1990)261.
28. Alexopolous, T. et al., E735 Collab., University of Notre Dame preprint, 1992.
29. I.Kawrakow, H.–J.Möhring and J.Ranft, *Z. Phys.* C56(1992)115.